Reduction crystallization of Ni, Cu, Fe and Co from a mixed metal effluent

T.P. Phetla, F. Ntuli *, E. Muzenda

University of Johannesburg, Department of Chemical Engineering, School of Mining, Metallurgy and Chemical Engineering, P.O. Box 17011, Doornfontein 2088, South Africa

ARTICLE INFO

ABSTRACT

Removal and recovery of heavy metals from effluent are major concerns due to diminishing fresh water resources, depletion of exploitable ores and human and environmental health concerns. The objective of this work was to efficiently recover heavy metals from effluent in their elemental form as metallic powder by reduction crystallization. This method recovers metals in a pure form and enables them to be directly used. Experiments were conducted using mixed metal solutions of Ni, Cu, Co, and Fe in a 20 L Perspex batch reactor using hydrazine as a reducing agent and nickel powder as seeding material. Ni, Cu, Co and Fe were effectively reduced to their elemental states with removal efficiencies of over 99% for Ni and Co and about 98% for Cu and Fe. Residual concentrations obtained for Ni, Co and Fe were below 0.05 mg/L and below 1.20 mg/L for Cu. Based on the evolution of the particle size distribution (PSD) and its derived moments the dominant particulate processes identified were aggregation, growth and breakage with the possibility of nucleation in the presence of Fe. However, particle size enlargement was largely due to aggregation.

1. Introduction

Wastewater treatment is becoming ever more critical due to diminishing water resources, increasing wastewater disposal costs and stricter discharge regulations that have lowered permissible contaminants levels in wastewater stream. Heavy metal laden wastewater produced by mining and mineral processing activities, e.g. acid mine drainage and process effluent occurs at an estimated 70% of world's mine sites, making it one of the mining industry's most significant environmental and financial liability. The fast depletion of exploitable mineral resources and negative impact these toxic metals have on human health and the environment necessitates the recovery of these metals. Thus, the removal and recovery of heavy metals from effluents has been a subject of significant importance. A number of treatment methods have been developed for heavy metal removal namely, precipitation, adsorption, ion-exchange and membrane technologies. Of these methods, precipitation is the widely used because it is the most economical method and easier to implement and operate on a large scale. However, traditional precipitation methods using lime, sulfides or hydroxides recover metals in the form of a sludge which is not reusable and has to be disposed in landfills creating a potential environmental hazard and resulting in loss of valuable mineral.

Due to the fast depletion of mineral reserves globally, the current focus in effluent treatment is now on the recovery and re-use of these heavy metals rather than removal and disposal. Of the methods currently in use none is capable of recovering metals in a form that is suitable for re-use hence there is a need to develop alternative technologies to address this problem. In this study, reduction crystallization method was investigated as a possible method for the removal and recovery of heavy metals.

In this method hydrazine was utilized as a reducing agent for the removal and recovery of the metals because the pH and temperature dependent reducing ability of hydrazine makes the reduction rate easily controllable [1]. Hydrazine is a strong reductant widely used in various chemical operations. A series of striking results has been obtained where hydrazine was used as a reducing agent for the production of finely divided metals, metal-on glass films, metallic hydrolysis and electro-less plating [2].
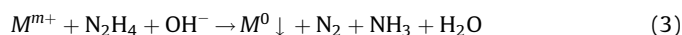
An important half reaction involving hydrazine is:

$$4OH^- + N_2H_4 \leftrightarrow N_2 + 4H_2O + 4e^- \quad (E = -0.31 - 0.06pH) \qquad (1)$$
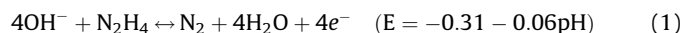
It can effectively be employed in the reduction of various metal cations (M^{n+}) to elemental state (M^0) according to the following reaction [3]:

$$M^{n+} + N_2H_4 \rightarrow M^0 \downarrow + N_2 + H^+ \qquad (2)$$

Based on the discussion by Tobe and Burgess in 1996 [4], metal ions can also be reduced:

$$M^{m+} + N_2H_4 + OH^- \rightarrow M^0 \downarrow + N_2 + NH_3 + H_2O \qquad (3)$$

* Corresponding author. Tel.: +27 11 5596003; fax: +27 11 5596430.
E-mail address: fntuli@uj.ac.za (F. Ntuli).
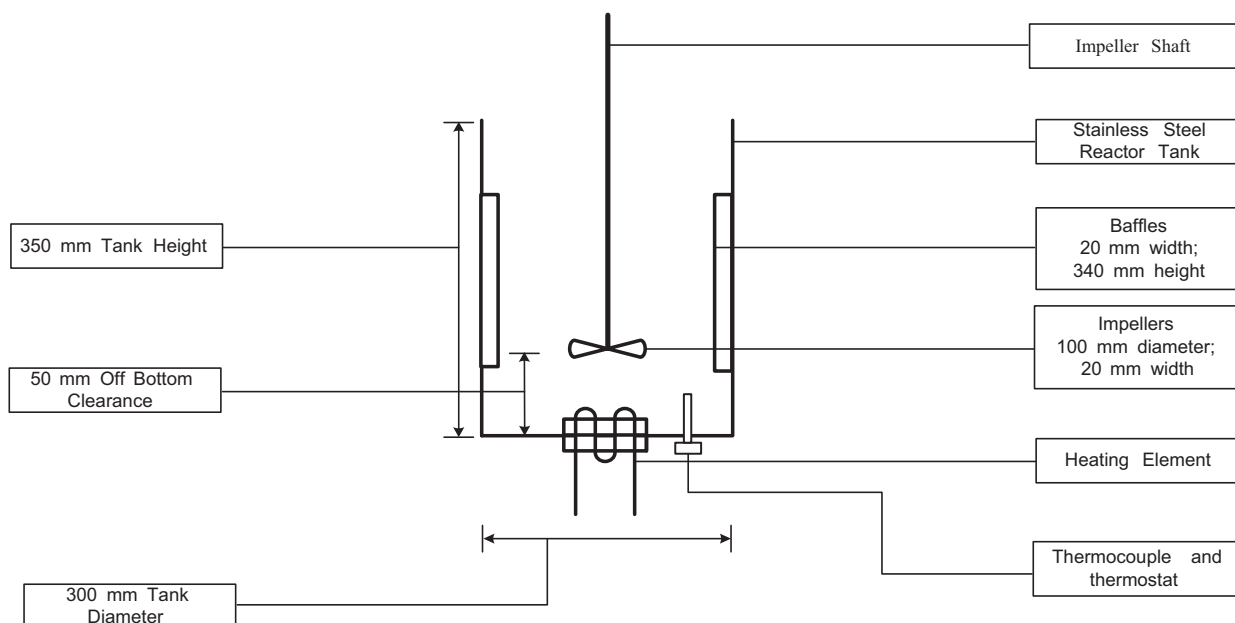
Fig. 1. Perspex batch reactor.

Hydrazine can react with dissolved oxygen (DO) in water according to [5]

$$N_2H_4 + O_2 \rightarrow N_2 + 2H_2O \tag{4}$$

Hydrazine can also undergo self oxidation and reduction in both alkaline and acidic solutions. The decomposition of hydrazine proceeds by Eq. (5):

$$3N_2H_4 \rightarrow N_2 + 4NH_3 \tag{5}$$

Precious metals can be easily recovered by using this powerful reductant, Eq. (2). Since metal cations are immediately reduced to metallic state, there is very limited amount of metal ions present in the solution. Complexation between metal and ammonia due to Eqs. (3) and (5) is therefore unlikely to occur. By using air stripping, ammonia is easily removed from the solution. In addition, unutilized hydrazine can be removed by aeration, Eq. (4). The reduction potential for all the metals investigated in this study are shown in Table 1, the reaction between metals and hydrazine is spontaneous; indicating that the actual experiments are thermo-dynamically feasible.

2. Experimental

2.1. Apparatus and reagents

Experiments were conducted using a 20 L Perspex batch reactor fitted with 4 baffles, a 4-pitched blade axial impeller with an off bottom clearance of 50 mm to ensure adequate solid suspension, a heating element, thermocouple and thermostat for temperature

Table 1
Reduction potential for Ni, Cu, Co and Fe.

Electrode reaction	Potential E (V (nhe))	Calculated reduction potential (V(nhe))
$Ni^{2+} + 2e^- = Ni$	−0.23	−0.74
$Cu^{2+} + 2e^- = Cu$	+0.337	−0.633
$Co^{2+} + 2e^- = Co$	−0.277	−1.247
$Fe^{2+} + 2e^- = Fe$	−0.440	−1.410
$Fe^{3+} + 3e^- = Fe$	−0.040	−1.010

control. A schematic representation of the reactor is shown in Fig. 1.

A pH meter was used to monitor pH, and 2 M sodium hydroxide as a pH regulator. Sulfate salts of nickel, copper, cobalt and iron were used to prepare the synthetic effluent solutions. 1 M hydrazine in tetra-hydrofuran was employed as a reducing agent and nickel powder supplied by Impala Platinum Refineries was used as seeding material.

2.2. Preparation of synthetic effluent solution

100 mg/L of synthetic solutions of each specific metal or a combination thereof were prepared by weighing 4.48 g of nickel sulfate hexahydrate, 4.77 g cobalt (II) sulfate heptahydrate and 3.929 g cupric sulfate by dissolving the salts into 1000 mL of water in a volumetric flask. 4.979 g ferrous sulfate was dissolved into 1000 mL of water to make 97.94 mg/L iron solution.

2.3. Experimental method

10 L of 100 mg/L of either Ni–Cu, Ni–Fe or Ni–Co synthetic solution was fed into a 20 L stirred batch reactor. To catalyze the oxidation of hydrazine and due to cost implication, 30 g of pure nickel powder was added into the reactor as seeding material. The seeding material was used to avoid nucleation in the experiments, to enable effective control of particle size distribution (PSD) and avoid having wide PSD. The solution was then heated to 45 °C and at this temperature 0.3 mL of 1 M hydrazine was added into the reactor, under 500 rpm constant stirring speed. Reduction crystallization proceeded under pH 10.7–11.0. 1 M sodium hydroxide solution was added at 60 °C to raise and maintain the pH within the given range. A reaction time of 3 min was used, since the reduction reaction is very rapid. After the reaction was complete, the agitator was switched off and the solution was allowed to cool. 5 mL aliquot of the reduced solution was sampled using a pipette; thereafter the reduced solution was discharged leaving behind the seed material. A fresh metal solution was then added and the process was repeated using the same procedure as outlined above. After three batch reductions the mixture of the reduced solution and

nickel powder was discharged from the reactor and filtered to obtain the nickel powder and the residual effluent. The powder sample was then washed with hot water and dried in an oven at 80 °C. Each experiment was repeated once to check for reproducibility of the results. Similar experimental conditions were used for all the three metal solutions (i.e. Ni–Cu, Ni–Fe and Ni–Co) as the main focus was not on selective removal of these metals. Therefore, the operating conditions were pH of 10.7–11.0 and temperature of 60 °C for all the experiments.

2.4. Characterization

Residual nickel, copper, cobalt and iron ion concentrations were measured by inductively coupled plasma-optical emission spectrometer (ICP-OES; model Spectro Arcos Fsh12). The Ni powder particle morphology was captured using a scanning electron microscope (SEM; model Jeol JSM 5600). The elemental composition of the powder was measured by X-ray fluorescence (XRF; model Magix Pro Phillips). Laser diffraction (Malvern Mastersizer 2000) coupled to a liquid dispersing unit (Hydro 2000G) was used to measure the PSD of the powder samples in order identify the particulate processes occurring during reduction crystallization.

3. Results and discussion

Each batch run is termed a densification because the powder becomes denser with each successive batch reduction. The results for the residual concentration of each metal, removal efficiency, reduction rate and evolution of the PSD and its derived moments are presented below.
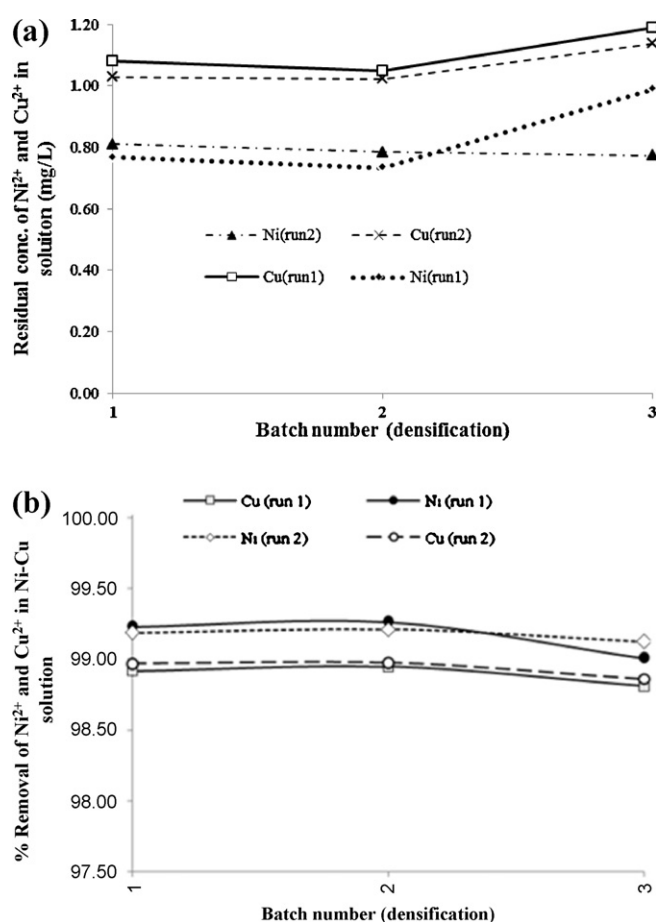
3.1. Residual concentration and removal efficiency

The residual nickel and copper concentrations and the removal efficiency of each respective metal with each successive densification are shown in Fig. 2.

The results clearly indicate an effective reduction of nickel and copper in the wastewater with increasing number of densifications (Fig. 2(a)). Copper residual concentration was higher than nickel residual concentration in Ni–Cu solution for all the densifications. The highest copper concentration was 1.19 mg/L and 0.99 mg/L for nickel from a 100 mg/L initial concentration of Ni and Cu. The lowest residual nickel and copper concentrations were 0.74 mg/L and 1.02 mg/L, respectively. The % of nickel removed was higher than that of copper with the exception of the 2nd experimental run at the 3rd densification (Fig. 2(b)). The highest % removal of Ni^{2+} and Cu^{2+} was obtained in the 2nd densification and decreased sharply with the increasing number of densifications. Removal of nickel from the effluent was generally favored over that of copper. Based on the reduction potential of Ni (-0.23) and Cu (0.34), the reduction of Cu is thermodynamically more favorable to that of Ni. However, from the results obtained Ni was preferentially removed when compared to Cu. Since Ni seed was used as seeding material it is proposed this favors the preferential deposition of Ni over Cu. Reusing nickel powder improved the recovery from the 1st densification to the 2nd densification and recoveries began to decline thereafter.

Fig. 3 shows the residual nickel and cobalt concentrations and the removal efficiency of each respective metal with each successive densification. The residual nickel concentration was higher than that of cobalt (Fig. 3(a)). The highest concentrations

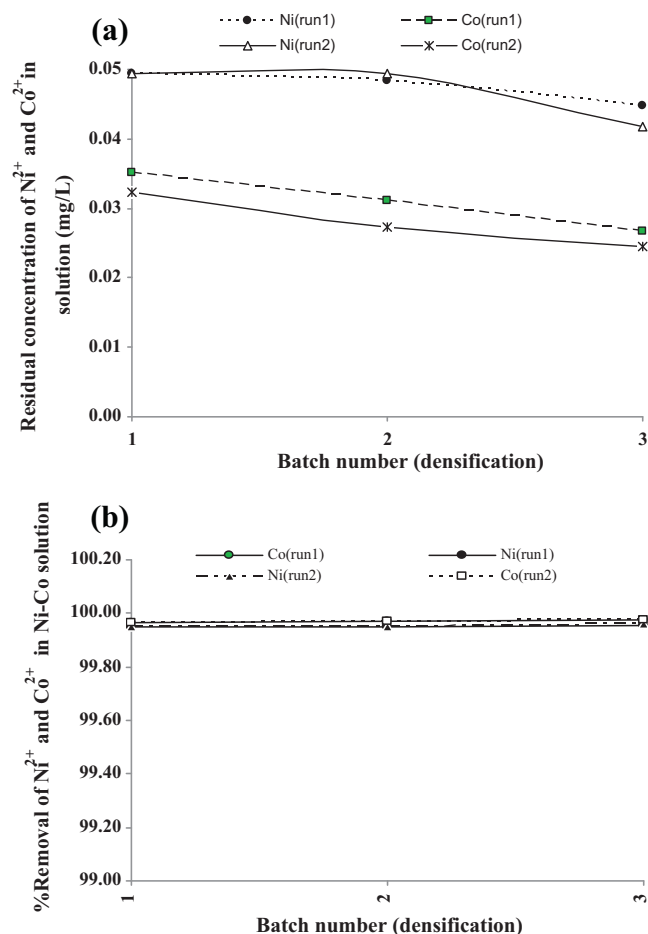Fig. 2. (a) Residual Ni and Cu concentration and (b) %removal from Ni–Cu solution.

Fig. 3. (a) Residual Ni and Co concentration and (b) %removal from Ni–Co solution.

were 0.039 mg/L and 0.035 mg/L for nickel and cobalt, respectively. Reusing the nickel powder as seed for subsequent densifications had a positive effect on metal recovery especially for cobalt as the residual concentration gradually decreased from 1st to the 3rd densification (Fig. 3(a)). The highest % removal for cobalt was 99.97% and 99.92 for nickel (Fig. 3(b)). The removal of nickel and cobalt were almost the same in all the densification but the removal of cobalt was favored over that of nickel with a difference of about 0.05%. The anomalous preference of cobalt co-deposition over nickel has been reported in previous electrodeposition studies. Even though the concentration of Ni in solution was higher than that of Co, the Co content in the alloy was higher than that of nickel. It was proposed that co-deposition of Ni–Co alloy catalyses the electrodeposition of Co and inhibits that of Ni, leading to a greater proportion of Co in the Ni–Co deposits [6].

Fig. 4 shows the residual nickel and iron concentrations and the removal efficiency of each respective metal with each successive densification. The residual concentration for both nickel and iron decreased with the increase in the number of densifications. The highest residual concentration was 0.032 mg/L and 0.047 mg/L for nickel and iron, respectively, in Ni–Fe solution, from initial concentration of 100 mg/L nickel and 97.94 mg/L iron (Fig. 4(a)). Generally, Fe^{2+} is difficult to be reduced into Fe directly in alkali aqueous solution, unless favored by some special measures (such as ultrasonic, high pressure, etc.). This is due to the electromotance of the oxidation reaction from Fe^{2+} to Fe^{3+} (0.66 V) which is higher than that of the reduction reaction from Fe^{3+} to Fe^{2+} (0.283 V). So Fe^{2+} is likely to be oxidized into Fe^{3+} [7].
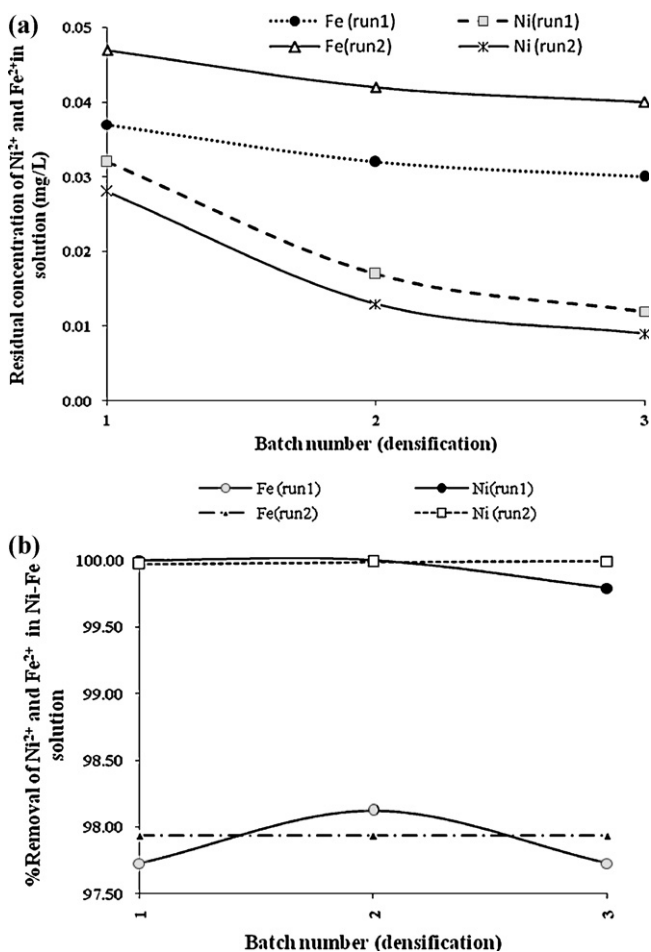
Removal efficiency was above 97.93% for iron and almost 100% for nickel in all densifications, making the % removal rate of nickel higher than that of iron (Fig. 4(b)). Previous studies have shown that nickel can accelerate catalytic decomposition of hydrazine because of its peculiar catalytic activity [8]. It is proposed that the existence of Ni^{2+} in the initial solution facilitates the reduction of Fe^{3+} to Fe resulting in the formation of Fe–Ni alloy particles. Furthermore, Ni could stabilize the Fe–Ni particles and hinder oxidization of Fe during the course of hydrazine reduction because of its higher stability compared with Fe. Reusing nickel seed had a minor effect on metal recovery from the 1st to 2nd densification.

3.2. Reduction rate

The reduction rate of each metal in its respective solution is shown in Fig. 5. The reduction rate of copper and nickel in the Ni–Cu solution generally increased from the 1st to the 2nd densification and decreased thereafter for copper (Fig. 5(a)). However, no clear trend was observed for nickel after the 2nd densification.

The rate of nickel and cobalt reduction from the Ni–Co solution increased from the 1st to 3rd densification for all the experimental
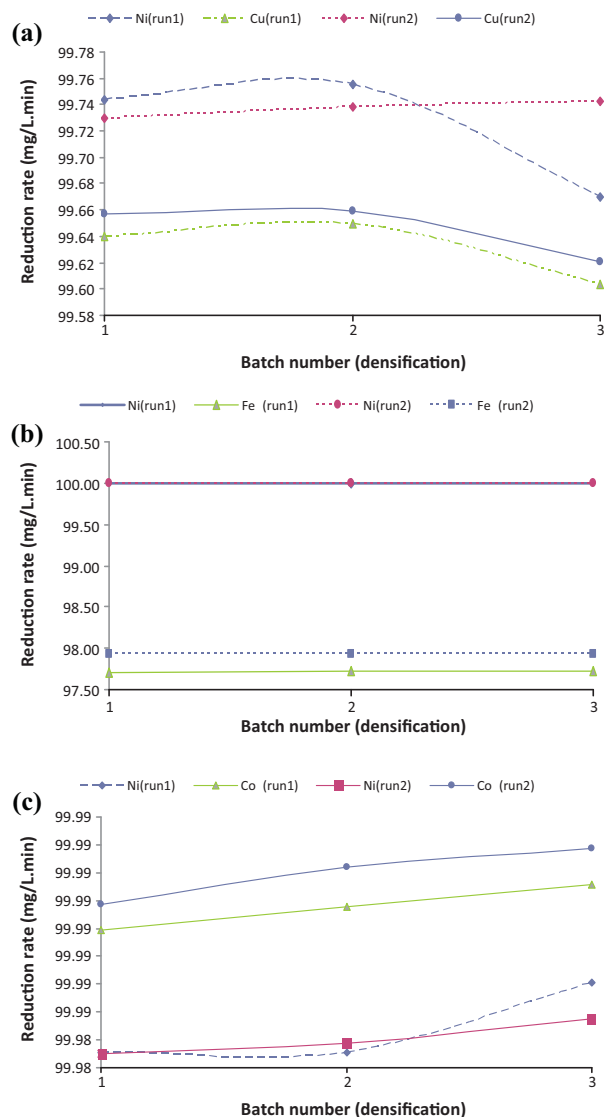
Fig. 4. (a) Residual Ni and Fe concentration and (b) %removal from Ni–Fe solution.

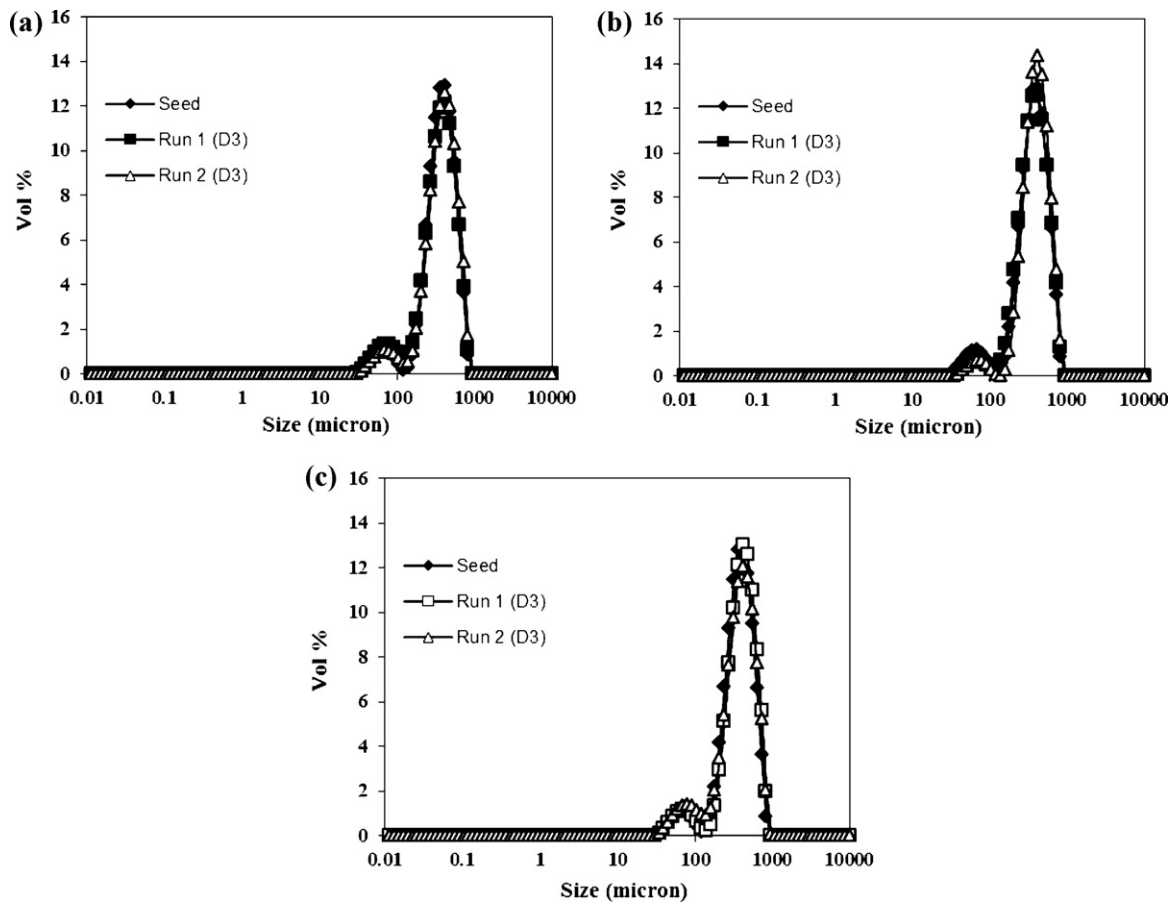**Fig. 5.** Reduction rate: (a) Ni–Cu solution, (b) Ni–Fe and (c) Ni–Co.

Fig. 6. Evolution of the PSD: (a) Ni–Cu, (b) Ni–Co and (c) Ni–Fe.

runs, indicating that the concentration of the metals removed increased with successive densifications (Fig. 5(b)).

There was no significant change in the reduction rate from the 1st to the 3rd densification with a change of about 0.002 mg/(L min) for nickel and 0.001 mg/(L min) for iron from the Ni–Fe solution (Fig. 5(c)).

The highest reduction rate was observed for Ni in the Ni–Fe solution, this agrees with previous studies where iron was found to act as a reduction catalyst in nickel reduction [9]. The lowest reduction rate was observed for Cu in the Ni–Cu solution. The co-deposition of nickel and copper also resulted in a decrease in the reduction rate of nickel when compared with the other metallic systems. This suggests that the presence of copper on the powder reduces the catalytic activity of the powder.

3.3. Evolution of the PSD and moments

Fig. 6 shows the evolution of the particle size distribution (PSD) of the powder obtained from the Ni–Cu solution, Ni–Co solution and Ni–Fe solution, respectively. From the evolution of the volume distribution it can be concluded that size enlargement was not significant as the modal size remained nearly unchanged (Fig. 6).

The PSD data was transformed into its moments using Eqs. (6) and (7):

$$n(L)\,dL = \sum_i \frac{\text{vol\%}_i \times \text{conc(vol\%)}}{100} \cdot \frac{1}{k_v \bar{L}^3} \tag{6}$$

$$m_j = \int_0^\infty L^j n(L)\,dL \tag{7}$$

The volume based histogram vol% versus L_i where i indicates the size sub-range and the particle concentration (vol%) were generated by laser diffraction (Malvern Mastersizer) and the volume shape factor k_v equal to $\pi/6$ was used. The first four moments (0th, 1st, 2nd and 3rd) are of special interest and are related to the total number, length, area and volume of solid per unit volume of suspension, respectively [10]. The 0th, 2nd and 3rd moments for the seed and the powder from the third densification is shown in Table 2. The average moments were generated by first creating an average of the two volume distribution curves from each experiment (Fig. 6) using Malvern software (Mastersizer 2000 Software) and then transforming the data into moments using Eqs. (6) and (7).

Comparing the 0th, 2nd and 3rd moments for the D3 powder to that of the seed shows that there was an increase in all the first three moments, corresponding to an increase in the number of particles, surface area and volume. The increase in particle number and surface area can be due to either nucleation or breakage or a combination of both mechanisms. The increase in the particle volume shows that growth of particles also occurred, however, this did not significantly affect the PSD since the mass deposited (approximately 1 g/densification) was very low relative to the number of particles (of the order of 10^{11}).

The D(4.3) and $\bar{L}_{1.0}$ of the powder after three densifications is shown in Table 3. The D(4.3) and $\bar{L}_{1.0}$ shows what happens to the larger sized particles of the PSD and the smaller sized particles, respectively. There was an increase in the D(4.3) and $\bar{L}_{1.0}$ of the powder produced after three densifications relative to the seed particles. The highest D(4.3) and $\bar{L}_{1.0}$ was obtained using the Ni–Co solution and the lowest D(4.3) and $\bar{L}_{1.0}$ values were obtained from the Ni–Cu and Ni–Fe solutions, respectively. The increases in the

Table 2
Moments of the PSD.

Sample	Moments		
	0th (# m^{-3} × 10^{11})	2nd (m^2 m^{-3} × 10^3)	3rd (m^3 m^{-3})
Seed	7.79	5.91	1.47
D3 powder (Ni–Cu)	12.93	8.24	2.00
D3 powder (Ni–Co)	10.40	7.83	1.93
D3 powder (Ni–Fe)	11.03	8.57	2.17

Table 3
Weighted mean sizes of the powder.

Sample	Weighted mean size (μm)	
	D(4.3)	$\bar{L}_{1.0}$
Seed	355.20	62.50
D3 powder (Ni–Cu)	357.81	66.40
D3 powder (Ni–Co)	376.31	89.95
D3 powder (Ni–Fe)	374.49	66.15

D(4.3) and $\bar{L}_{1.0}$ shows size enlargement by particle aggregation. Thus, molecular growth mainly served to provide a metallic bridge to cement (or glue) the particles together. Therefore, the dominant particulate processes identified in all the experiments were aggregation, growth and breakage. Evidence of the occurrence of nucleation was only observed for the experiments conducted using the Ni–Fe solution.

3.4. SEM of nickel powder and powder purity

The morphology of the nickel powder produced using Ni–Cu, Ni–Co and Ni–Fe solution is shown in Fig. 7. The SEM micrograph of the powder produced in all the experimental runs exhibited a nearly spherical structure with wide distribution in particle size. There was also evidence of particle fragmentation indicating that the increase in particle number and surface area was largely due to breakage rather than nucleation. However, the SEM micrograph of the powder produced in Ni–Fe solution (Fig. 7(c)) reveals a large proportion of smaller particle fragments. Given the size of some of these fragments and the fact that Fe has been found to act as a nucleating agent even in buffered solutions [9], it is possible that nucleation might have contributed to their generation.

Table 4
Elemental composition of the powder.

Sample	Concentration (%)
Seed	98.38
D3 powder (Ni–Cu)	
Ni	99.40 ± 0.01
Cu	0.40 ± 0.01
D3 powder (Ni–Co)	
Ni	99.55 ± 0.04
Co	0.42 ± 0.04
D3 powder (Ni–Fe)	
Ni	99.59 ± 0.06
Fe	0.19 ± 0.03

Table 4 shows the elemental composition of the powders obtained from each respective metal solution. The nickel content of the powder increased from that of the seed as a result of nickel plating from solution. Since nickel powder was used as seeding material nickel was the predominant element in all the powders produced. The iron content in the powder was almost half the amount when compared to the content of copper and cobalt when crystallized from their respective solutions with nickel. Some of
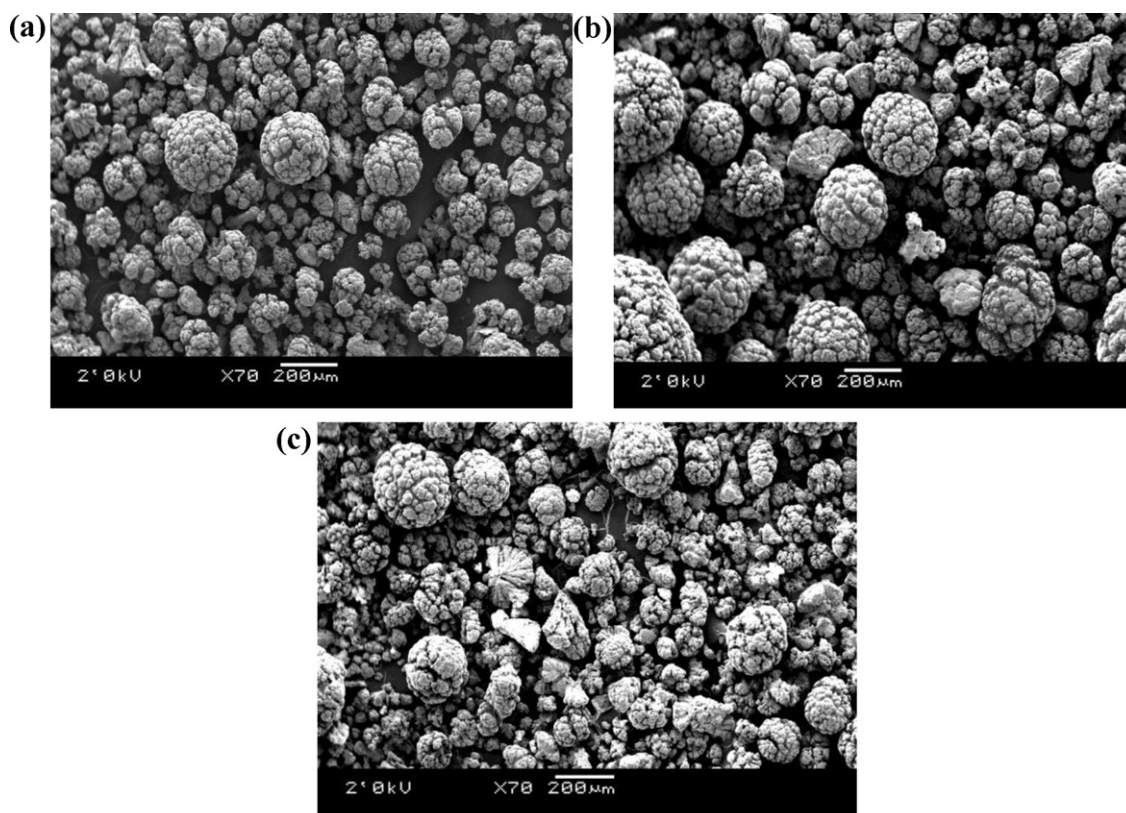

Fig. 7. Scanning electron micrographs of D3 powder: (a) Ni–Cu, (b) Ni–Co and (c) Ni–Fe.

the iron might have been removed as a ferric hydroxide precipitate together with a small amount of colloidal precipitate generated.

4. Conclusions

The results obtained indicate that hydrazine is an effective agent to crystallize Ni, Cu, Co and Fe into their elemental states with nickel powder as a seeding material with removal efficiencies of over 99% for Ni and Co and about 98% for Cu and Fe. %Ni removal was highest in the presence of Fe due to its ability to act as reduction catalyst and lowest in the presence of Cu. The deposition of Cu on the seed was found to lower its catalytic activity and deposition of Ni was more favorable to that of Cu despite the fact that the reduction of Cu is thermodynamically more favorable to that of Ni. Cobalt deposition was more favorable to that of nickel with a difference of about 0.05% and cobalt co-deposition was found to inhibit nickel reduction and catalyzed cobalt reduction. Reusing the nickel powder seeding material for subsequent batch reductions resulted in lower residual metal concentrations for Ni, Co and Fe.

Based on the evolution of the volume distribution and the 0th, 2nd and 3rd moments the dominant particulate processes identified were aggregation, growth and breakage. Evidence of the possibility of nucleation was only found in the presence of Fe. Size enlargement was mainly due to aggregation, growth served to provide the crystalline bridge to cement the particles together. The residual concentrations obtained for Ni, Co, Fe were below 0.05 mg/L and only exceeded 1 mg/L for the Ni–Cu solution. Based on these results, reduction crystallization can be effectively used to recover heavy metals from effluent in their elemental form.

References

[1] G. Huang, S. Xu, X. Gang, L. Li, L. Zhang, Transactions of Nonferrous Metals Society of China 19 (2009) 289–393.
[2] D.K. Simpson, Metal Finishing 83 (1985) 57–60.
[3] J.P. Chen, L.L. Lim, Chemosphere 49 (2002) 363–370.
[4] M.L. Tobe, J. Burgess, Inorganic Reaction Mechanism, Prentice Hall, New Jersey, 1999.
[5] I.F. Audrieth, B.A. Ogg, The Chemistry of Hydrazine, John Wiley and Sons, New York, 1951.
[6] E. Gomez, E. Pellicer, E. Valles, Journal of Electroanalytical Chemistry 580 (2005) 222–230.
[7] X. Lu, G. Liang, Y. Zang, Materials Science and Engineering B 139 (2007) 124–127.
[8] Y.D. Li, L.Q. Li, H.W. Liao, H.R. Wing, Journal of Materials Chemistry 9 (1999) 2675–2677.
[9] F. Ntuli, A.E. Lewis, Chemical Engineering Science 62 (2007) 3756–3766.
[10] F. Ntuli, A.E. Lewis, Chemical Engineering Science 64 (2009) 2202–2215.